ISSN 2070-0482, Mathematical Models and Computer Simulations, 2021, Vol. 13, No. 1, pp. 91–105. © Pleiades Publishing, Ltd., 2021.
Russian Text © The Author(s), 2020, published in Matematicheskoe Modelirovanie, 2020, Vol. 32, No. 6, pp. 3–20.

LES-based Computation of Evolution of Turbulent Wakes Subjected to Adverse Pressure Gradient

E. K. Guseva[a], M. Kh. Strelets[a, *], A. K. Travin[a], and M. L. Shur[a]

[a] *Peter the Great Saint-Petersburg Polytechnic University, Saint-Petersburg, Russia*

**e-mail: strelets@mail.rcom.ru*

Received October 21, 2019; revised October 21, 2019; accepted November 25, 2019

Abstract—Results are presented of scale-resolving computations of mean and turbulent (including the dissipation rate of turbulent kinetic energy) characteristics of the turbulent wake of a flat plate subjected to adverse pressure gradient (APG). The computations are performed in the framework of a zonal RANS-LES model for two configurations. In the first one, APG is created by a plane symmetric diffuser and in the second one by a system of two pairs of thin liner foils specially designed for this purpose. In the both cases a volumetric synthetic turbulence generator is used for creating turbulent content at the inlet of LES subdomain. High accuracy of results of the simulations is supported by their weak sensitivity to grid-refinement. Obtained detailed data on wakes' characteristics may be used for validation and improvement of RANS turbulence models as applied to the considered class of flows.

Keywords: turbulent wake of flat plate, adverse pressure gradient, zonal RANS-LES computations

DOI: 10.1134/S2070048221010099

1. INTRODUCTION

A deeper insight into the physics of turbulent near wakes subjected to the adverse pressure gradient (APG) and a reliable prediction of the characteristics of such wakes are essential for solution of many important aerodynamic problems. This is particularly the case for a problem of optimization of high-lift wings of modern commercial airplanes at low speed, i.e., during take-off and landing, when the wakes of the slat and of the main wing are subjected to APG created by the flow past the flap. The presence of the APG leads to increase of the wake width and to emergence of a stagnation region or even of a local reversal flow region also known as "off-body separation" zone (see Fig. 1). This, in turn, leads to decrease of the effective angle of the wake direction and to a limitation of the maximum lift of a wing.

As shown in a number of studies (see, e.g. [1–3]), these complex phenomena unfortunately cannot be captured by existing cost-effective RANS turbulence models which for many years have been used successfully for design and optimization of parameters of high-lift wings at the cruise flight. On the other hand, employing high-fidelity eddy-resolving approaches based on the large eddy simulation (LES) for optimization purposes is virtually impossible because of their excessively high computational cost. Nevertheless, computational resources available already today allow using these methods for obtaining detailed quantitative data on the mean and the turbulent characteristics of the wakes subjected to APG. These data, along with results of measurements, may be used for validation and improvement of RANS turbulent models for the class of flow in question. It should be noted in this respect that using for this purpose reliable numerical predictions is, in a sense, preferable, because an objective evaluation of RANS models capabilities by means of comparison with experiments is often complicated or even impossible due to the complexity of exact reproducing the experimental environment in the computations. Besides, even if the most informative modern experimental techniques, e.g. particle image velocimetry (PIV), are used, some key characteristics required for an improvement and calibration of RANS turbulence models cannot be measured. This is especially relevant to the rate of viscous dissipation of the turbulent kinetic energy and the Reynolds stresses.

These considerations motivated the present study which was performed in the framework of a joint German–Russian project "Wake Flows in Adverse Pressure Gradient".

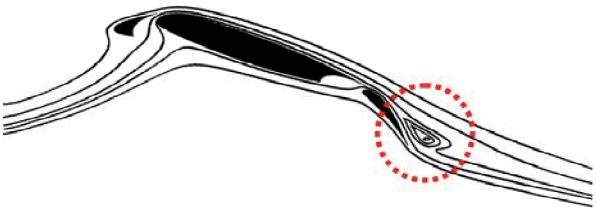

Fig. 1. Sketch of high lift wing with off-body separation zone at take-off and landing stages.

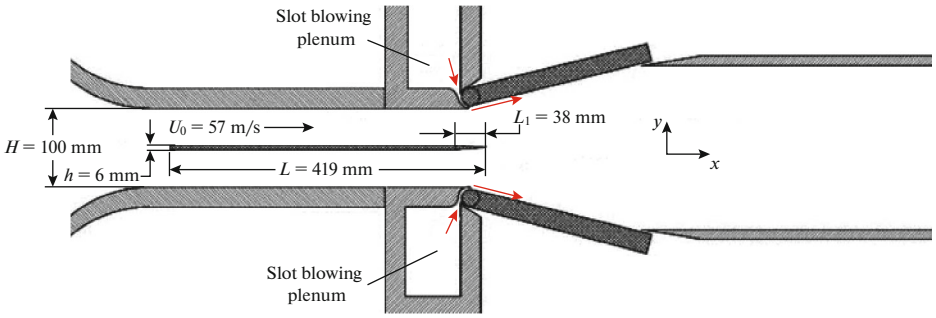

Fig. 2. Schematic of experimental rig [2] for investigation of flat plate wake subjected to APG.

In Section 2 of the paper, numerical setups are presented of the two specific wakes generated by a flat plate and subjected to APG. In both cases a zonal approach to turbulence representation is employed. In particular, in the initial part of the flat plate, RANS is used, while further downstream (in the downstream part of the plate and in the near wake) wall-modeled LES (improved delayed detached eddy simulation, IDDES [4]) is applied. Then, in Section 3, some aspects of the numerical implementation of this approach for the considered flows are presented. Finally, Section 4 provides main results of the performed simulations.

2. CONSIDERED MODEL FLOWS AND CORRESPONDING NUMERICAL PROBLEMS SETUPS

As mentioned in the Introduction, two flows with different methods of creating the APG were considered.

The first one is similar to the flow studied in the experiments [2] where the wake of the flat plate was subjected to APG created by a plane diffusor installed downstream of the trailing edge of the plate (Fig. 2).

Unfortunately, a full reproduction of the experimental setup in the simulations is impossible because of lack of the information on the characteristics of sonic jets injected into the boundary layers on the diffusor walls in order to avoid the separation caused by APG. So, a standing alone computational problem (Problem 1 hereafter) was formulated, which setup within the zonal RANS-IDDES approach is illustrated by Fig. 3. As seen in the figure, the only difference of this computational problem and the experimental configuration consists in replacement of the upper and lower hard walls of the test section by the "slip" walls, on which the nonpermeability and the free-slip boundary conditions are imposed ($v_n = 0$ and $\partial v_\tau / \partial n = 0$). In this way, a possibility of the separation of the boundary layer there is excluded. All the other parameters of the computational setup reproduce the corresponding experimental parameters. In particular, the flat plate thickness, h, equals 6 mm, its length is 419 mm, the radius of the flat plate leading edge is 3 mm, the height of the inlet section is 106 mm, the diffusor expansion ratio is 2.25, and the inlet velocity $U_{\text{ref}} = 57$ m/s, which corresponds to the Reynolds number based on the flat plate length 10^7.

Figure 3 also shows the position of the volume synthetic turbulence generator (VSTG) [5], which is used in the simulations to create artificial turbulence at the inlet of the IDDES subdomain ($x = -0.1$ m)

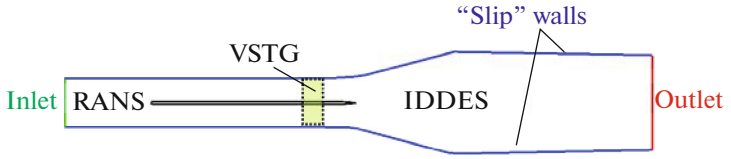

Fig. 3. Configuration of computational domain and of its RANS and IDDES subdomains, location of the volume generator of synthetic turbulence VSTG, and types of boundaries in Problem 1.

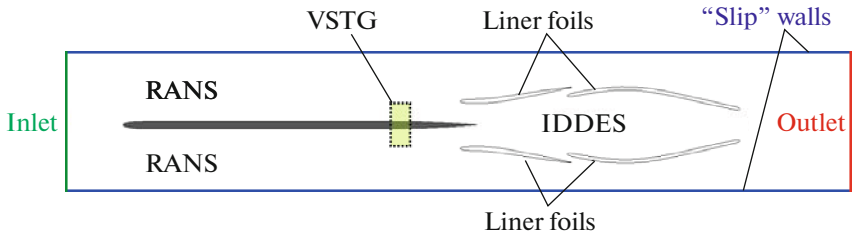

Fig. 4. Configuration of computational domain and of its RANS and IDDES subdomains, location of the volume generator of synthetic turbulence VSTG, and types of boundaries in Problem 2.

needed to ensure a rapid transition from fully-modeled turbulence in the RANS subdomain to mostly-resolved turbulence in the IDDES subdomain.

The flow is considered as incompressible. In the RANS subdomain, the k–ω SST turbulence model [6] is used, which also serves as an underlying RANS model in the IDDES.

The boundary conditions are specified as follows.

At the flat plate walls, the nonslip boundary conditions for velocity ($v_n = 0$ and $v_\tau = 0$) are used, the turbulent kinetic energy, k, is set zero, and its specific dissipation rate is computed as $\omega_w = 10\dfrac{6\nu}{\beta_1 \Delta y_1^2}$, where ν is the kinematic molecular viscosity, $\beta_1 = 0.075$ is the empiric constant of the SST model, and Δy_1 is the size of the first near-wall grid step [6].

At the inflow boundary of the computational domain located $25h$ upstream of the leading edge of the flat plate, uniform profiles of the velocity, k, and ω are imposed with the values of k and ω equal to $10^{-5}U_{\text{ref}}^2$ and $10U_{\text{ref}}/h$ correspondingly. This ensures fully turbulent boundary layer on the flat plate. Finally, the pressure at the inflow boundary is computed by the linear extrapolation from the interior of the domain.

At the outflow boundary located $100h$ downstream of the flat plate trailing edge, all the variables, except for the pressure, are linearly extrapolated from the interior of the domain, and the pressure is assumed to be constant.

Finally, the span size of the computational domain is equal to $5h$, and the periodic boundary conditions are imposed at $z = 0$ and $z = 5h$.

The second wake flow model considered in the present study reproduces the experimental model investigated in the experiments carried out in the framework of the already mentioned German–Russian project aimed at getting reliable experimental and numerical data on characteristics of turbulent wakes subjected to APG. A schematic of the flow (Problem 2 hereafter) is shown in Fig. 4. A principal difference of this configuration and that used in [2] consists in creating the APG by two pairs of specially designed thin liner foils. Thanks to this, even at strong values of APG leading to formation in the wake of virtually stagnant or off-body recirculation region, a possibility of separation of the boundary layers from the liner foils is eliminated without using any separation-control tools. This, in turn, allows complete reproducing the experimental conditions in the simulations. The geometrical and the regime parameters of the con-

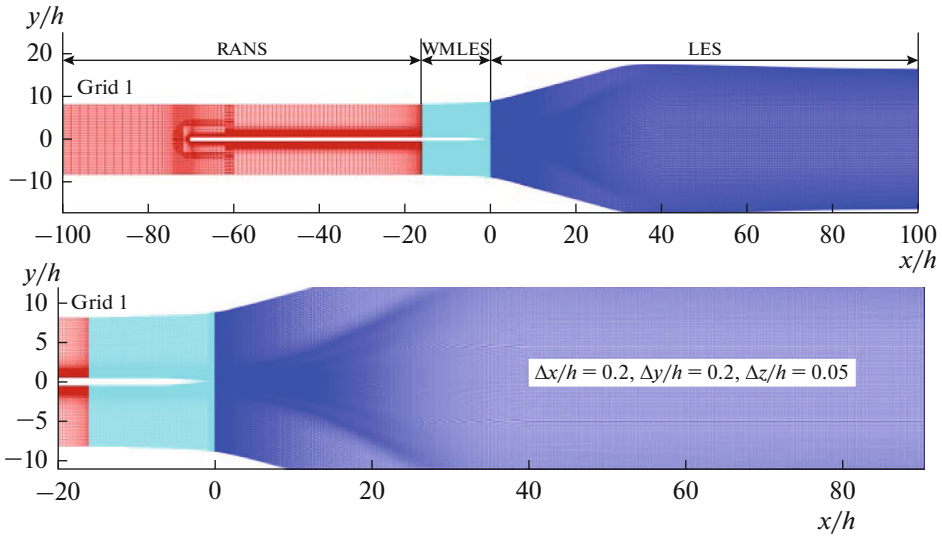

Fig. 5. Baseline grid (Grid 1) in *XY* plane for Problem 1 and its zoomed in fragment.

sidered flow model are described in details in [7]. Although experimental data for this configuration have not been obtained yet, results of its RANS-IDDES computation presented below have a significant value in themselves.

The boundary conditions used for solution of the Problem 2 are basically the same as those outlined above for the Problem 1. The only difference is that in this case the nonslip boundary conditions are imposed not only at the flat plate but also at the walls of the liner foils. Also similarly to the Problem 2, the span size of the computational domain is set equal to 5 thicknesses of the flat plate h.

3. NUMERICAL APPROACH

The numerical solution of the two problems described above was carried out in the framework of the unsteady 3D problem statement with the use of the own finite-volume CFD code of the St.-Petersburg Polytechnic University "Numerical Turbulence Simulation" (NTS code) [8]. It accepts structured Chimera-type grids with overlapping blocks. The incompressible branch of the code used in the present simulations employs the flux-difference splitting method of Rogers and Kwak [9]. In the RANS subdomain the inviscid fluxes are approximated with the use of the 3rd-order upwind-biased scheme, and in the IDDES subdomain, the 4th-order central scheme is applied. The viscous fluxes in both subdomains are approximated with the 2nd-order central scheme. For the time integration, an implicit three-layer backward scheme of the 2nd order of accuracy with subiterations in pseudo-time is applied. At the iterations, the system of discrete linear equations is solved using the Gauss–Seidel relaxation method over planes.

4. COMPUTATIONAL GRIDS

A baseline grid in *XY*-plane (Grid 1) used for Problem 1 is shown in Fig. 5. It consists of three main blocks. The first block covers RANS subdomain of the flat plate (RANS block) and the second one is aimed at computing its remaining part which is treated by IDDES functioning as Wall Modeled LES (WMLES block) there. Finally, the last, third, block covers the wake where IDDES functions as pure LES (LES block).

The grid in the RANS block is built based on well-known guidelines for computations with the use of the low-Reynolds RANS turbulence models.

The longitudinal grid step, Δx, in the WMLES block is equal to $\delta_0/8$ ($\delta_0 = 0.8h$ is the thickness of the boundary layer at the inlet section of this block, $x = -16h$). The grid step in the y-direction is exponentially

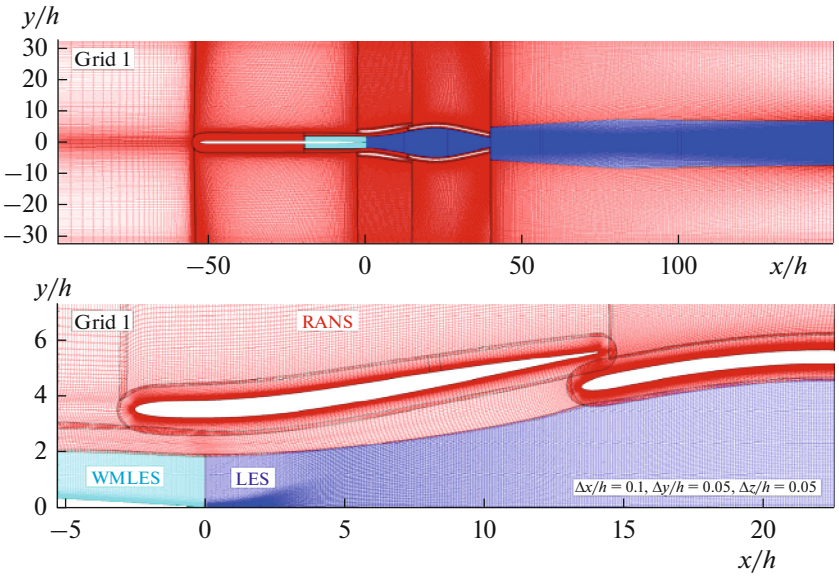

Fig. 6. Baseline grid (Grid 1) in *XY* plane for Problem 2 and its zoomed in fragment.

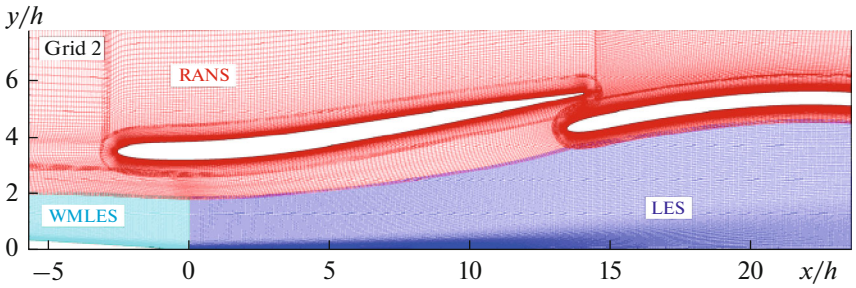

Fig. 7. Zoomed in fragment of refined grid (Grid 2) in *XY* plane for in Problem 2.

refined towards the wall and its first near-wall value in the law of the wall units, Δy_1^+, just as in the RANS block, is less than 1.0. The maximum grid step in y-direction is set to $0.2h$. Finally, the grid steps in the x- and y-directions in LES block covering the wake region, which is the focus of the study, are equal to $0.2h$.

The grid in the z-direction is uniform and has steps equal $0.5h$ in the RANS subdomain and $0.05h$ in the IDDES subdomain, respectively. As a result, a total size of the baseline grid is about 18 million.

In order to estimate the effect of the grid resolution on results of the simulations, along with the simulations on the baseline grid, similar simulations were conducted on two other grids (Grid 2 and Grid 3), which have the same topology but are considerably (1.4 and 2 times, respectively) refined compared to the baseline grid in the wake region in both the x- and y-directions. As a result, Grid 2 has about 28 million cells and Grid 3 has about 48 million cells.

The baseline grid in *XY*-plane used for the Problem 2 is shown in Fig. 6 (Grid 1 in the figures below). It is built using the same principles as those outlined above for the Problem 1. However, because of the more complex geometry, the grid has more blocks and, particularly, includes four O-type RANS blocks around the liner foils. In the WMLES region, the grid steps Δx and Δz are equal to 2×10^{-3} m and 10^{-3} m, respectively ($\Delta x/\delta_0 = 0.13$, $\Delta z/\delta_0 = 0.06$, where δ is the thickness of the flat plate boundary layer at the WMLES inlet). The near-wall grid step in the y-direction is 3×10^{-6} m, which, like in the Problem 1,

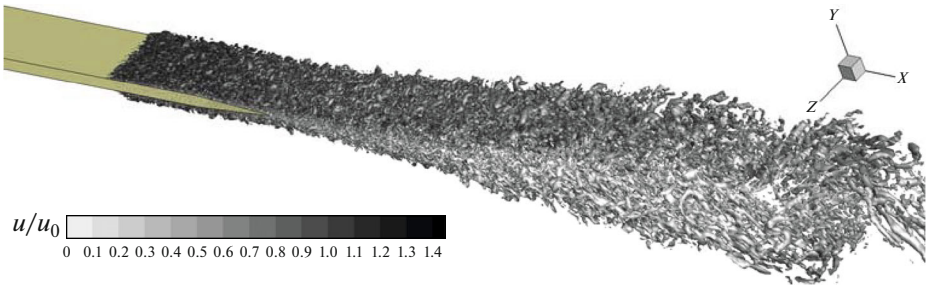

Fig. 8. Isosurface of swirl quantity λ (second eigenvalue of velocity gradient tensor) colored by streamwise velocity.

ensures less than 1.0 value of the nearest to the wall y-step in the wall units. As a result, the total number of cells in the baseline grid for the Problem 2 is about 28 million.

In addition to the baseline grid simulations, some additional simulations were performed on the grid with 1.6 times reduced steps in both the x- and y- directions (see Fig. 7). The size of this grid (Grid 2) is equal to 53 million cells.

5. RESULTS OF SIMULATIONS

5.1. Problem 1

Major results of this problem solution are presented in Figs. 8–14.

Figure 8 visibly displays the vortical structure of the flow downstream of the RANS-IDDES interface from the simulation on Grid 1. It reveals a rapid formation of developed 3D turbulent structures in the boundary layer on the plate and the existence of the virtually stagnant ("dead water") region in the central part of the wake.

Figure 9 compares the instantaneous fields of vorticity magnitude and eddy viscosity in an XY plane of the flow from the simulations performed on the three grids described above. The comparison suggests that with the grid refinement, consistently with the LES concept, more and more fine structures are resolved and the eddy viscosity significantly (by about an order of magnitude) drops, thus confirming plausibility of the IDDES functioning in the LES-mode. Other than that, a striking feature of these fields revealed by the figure is the instability of the wake and onset of its large-scale oscillations at $x/h > \approx 45$. This behavior excludes a possibility of predicting the wake characteristics in this area by a steady RANS model of any level of complexity. However, upstream of this section, the wake remains globally stable and accurate prediction of its characteristics there in the RANS framework is, in principle, possible.

Figures 10–12 give solid quantitative evidences in favor of high accuracy of the simulations. In particular, Fig. 10 suggests that even on the coarsest Grid 1, the turbulence spectrum has an extended (of the order of one decade) inertial range, and Fig. 11 demonstrates that simulations ensure resolution of about 90% of the turbulent kinetic energy. Finally, Fig. 12 suggests that in the wake area where it remains globally stable ($x/h < 45$), the prediction of the mean streamwise velocity is virtually grid-independent and captures the presence of the zone with nearly zero velocity.

In contrast to this, as could be expected keeping in mind that even in the finest of the considered grids (Grid 3) the step sizes far exceed the Kolmogorov length scale η ($\overline{\Delta \approx 75\eta}$), the rate of the kinetic energy dissipation directly computed according to its definition $\varepsilon = 2\nu\overline{S'_{ij}S'_{ij}}$ (S'_{ij} are the fluctuations of the components of the strain rate tensor) turns out to be highly grid-sensitive and, as seen in Fig. 13, the computations on the three considered grids do not reveal even a trend to grid convergence.

For this reason, the rate of the kinetic energy dissipation was computed with the use of an alternative method proposed in [10]. It consists in the evaluation of ε based on the balance of other terms of the kinetic energy transport equation, which, unlike the dissipation term, may be accurately computed based on reliable LES solution. Results of such computations shown in Fig. 14 suggest that even on the Grid 1, thus computed ε is virtually grid-independent. Same conclusion was drawn regarding the individual components of the dissipation rate tensor computed based on the balance of terms of the transport equations

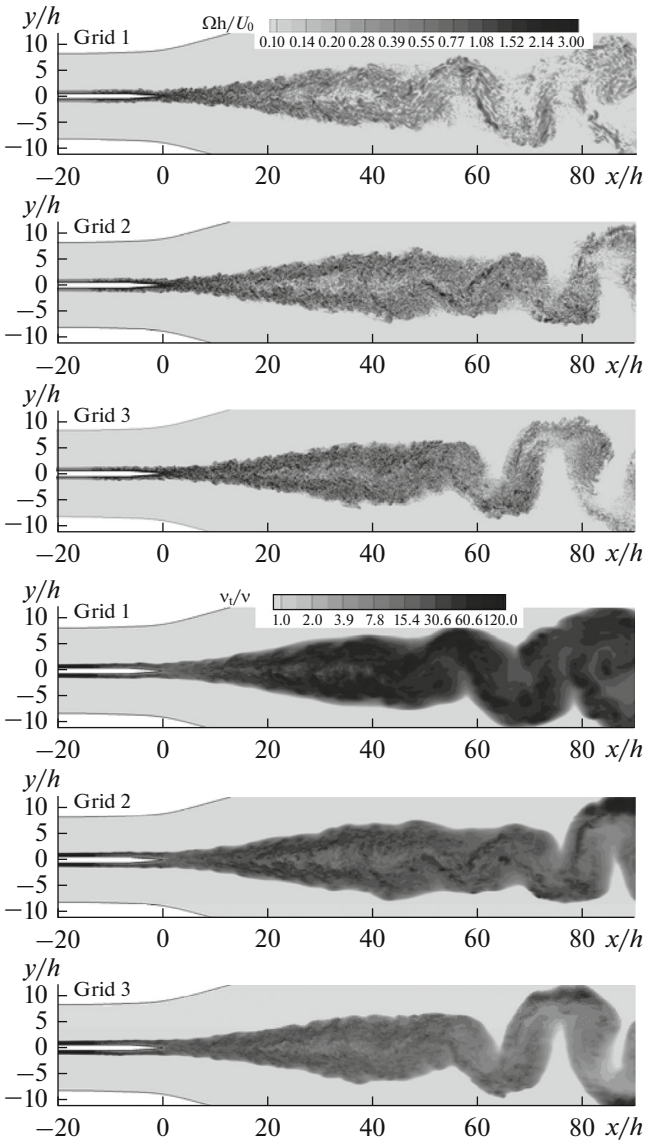

Fig. 9. Instantaneous fields of vorticity magnitude (upper frames) and subgrid viscosity (lower frames) from solution of Problem 1 on three progressively refined grids.

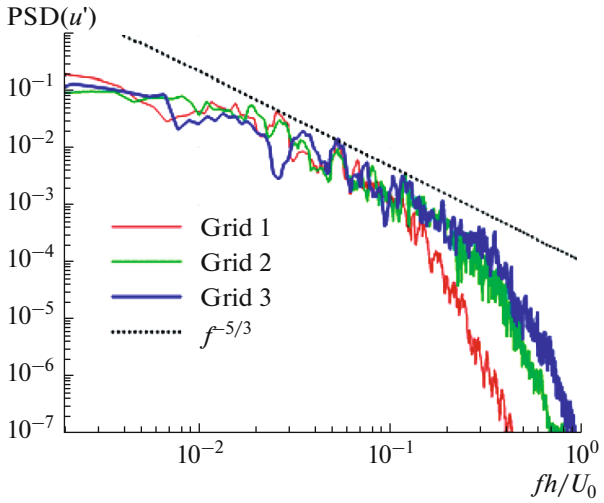

Fig. 10. Effect of grid-refinement on turbulence spectrum in section $x/h = 30$.

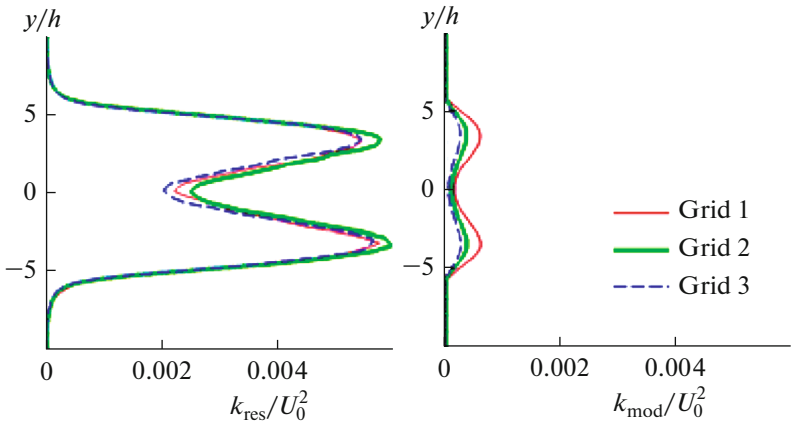

Fig. 11. Effect of grid on profiles of resolved (left) and modeled (right) turbulent kinetic energy in section $x/h = 35$.

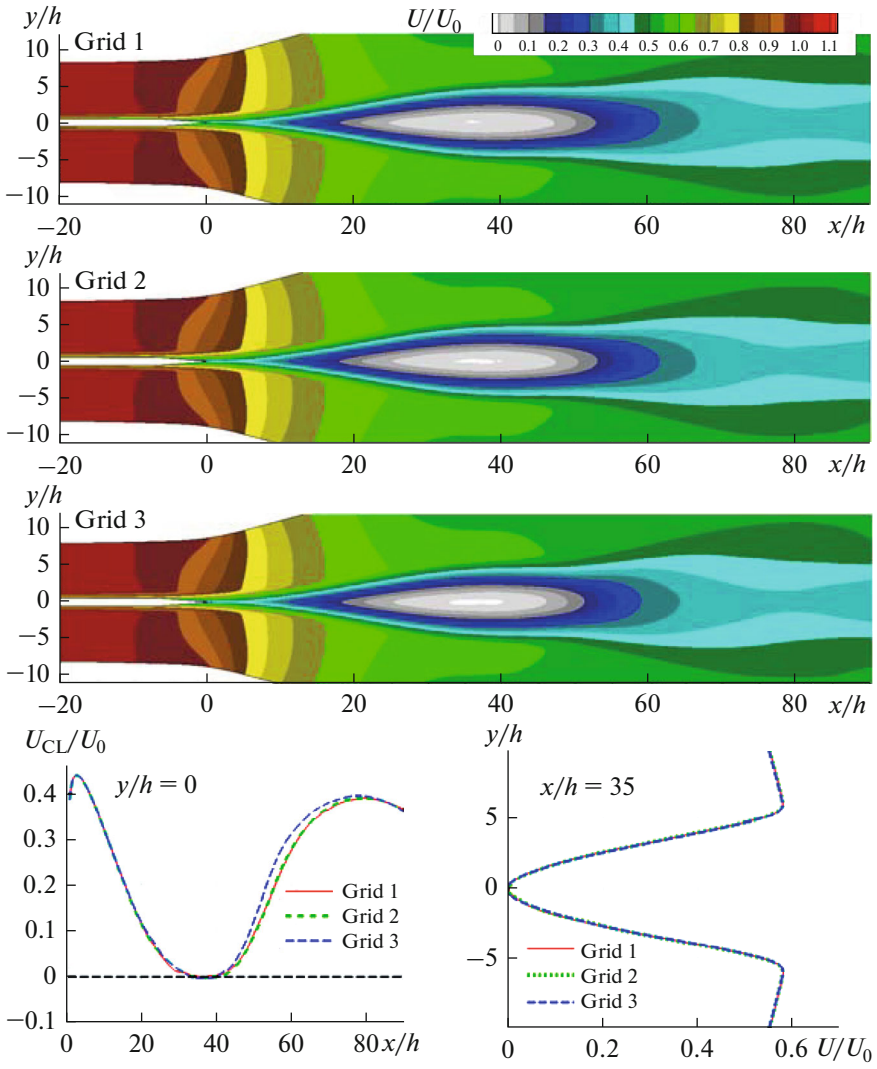

Fig. 12. Effect of grid-refinement on mean streamwise velocity field (upper frames), on its distribution along the wake symmetry plane ($y = 0$), and profile in section $x/h = 35$.

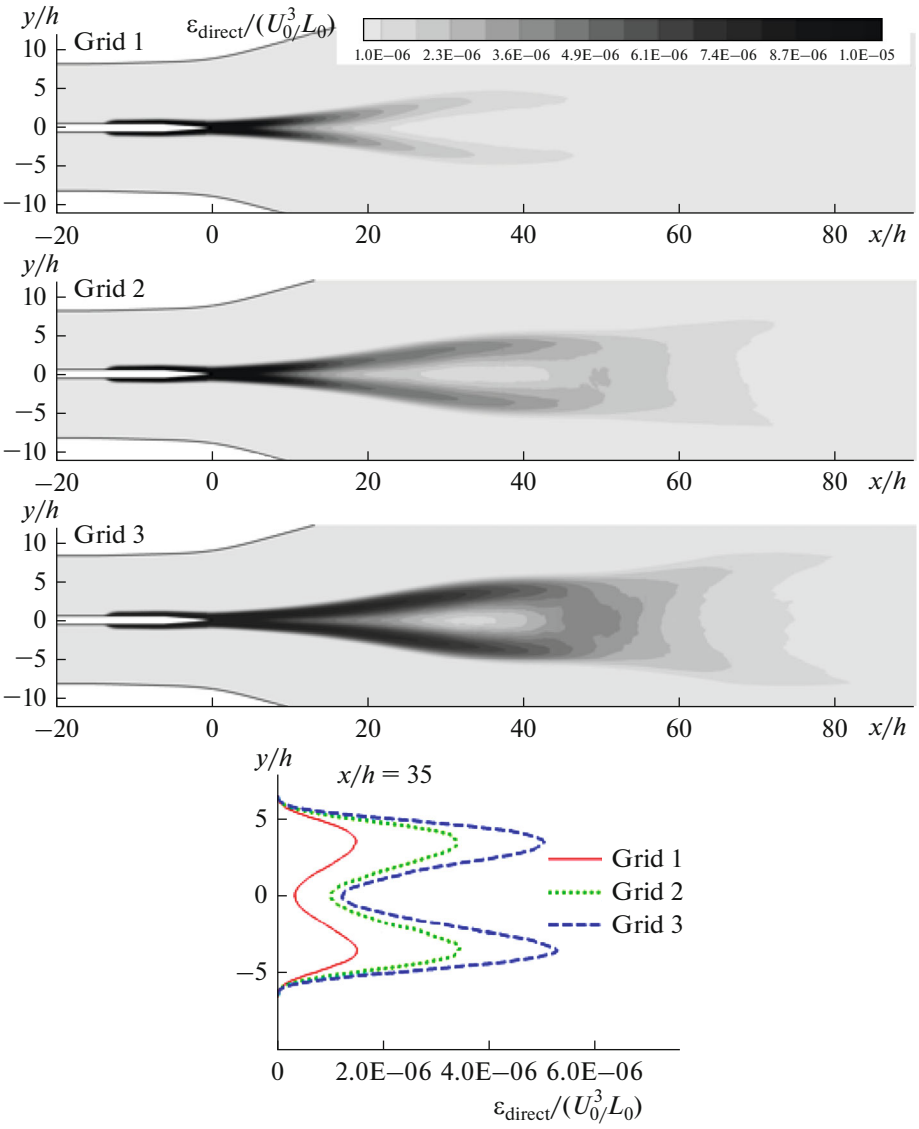

Fig. 13. Effect of grid-refinement on directly computed field of viscous dissipation rate of kinetic energy (upper frames) and on its profile in section $x/h = 35$ (lower frame).

for the components of the Reynolds stress tensor. These conclusions are rather important since, as mentioned above, the viscous dissipation rate, which is the key quantity for validation and improvement of RANS turbulence models, cannot be measured with sufficient accuracy in the experiments.

As far as physical peculiarities of the wake in APG at the considered flow parameters are concerned, a primary one is a large velocity deficit in the wake: as seen in Fig. 12 above, the velocity in its symmetry plane drops to almost zero. However, at these parameters, a reversal flow region ("off-body separation") is not observed.

5.2. Problem 2

Main results obtained for this problem at the Reynolds number based on the plate length equal 1.6×10^6 and at the distance between the upper and lower liner foils and the symmetry plane equal to 7 cm ($3.5h$) are shown in Figs. 15–20.

In particular, Figs. 15–17 show that, similar to what is observed for the Problem 1 (see Figs. 8–10), the simulations ensure a rapid formation of developed 3D turbulent structures in the WMLES region of the

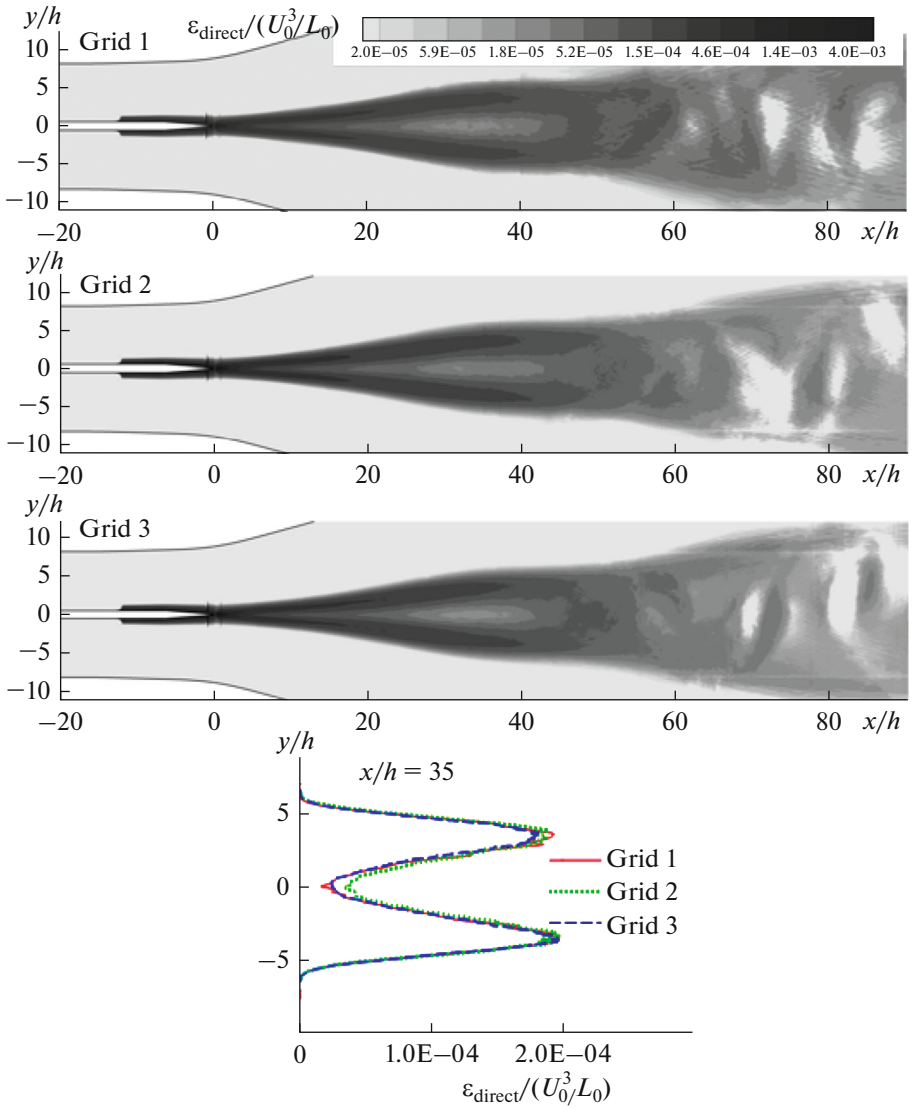

Fig. 14. Same, as in Fig. 13, for the rate of viscous dissipation computed based on the balance of the terms of the turbulent kinetic energy transport equation.

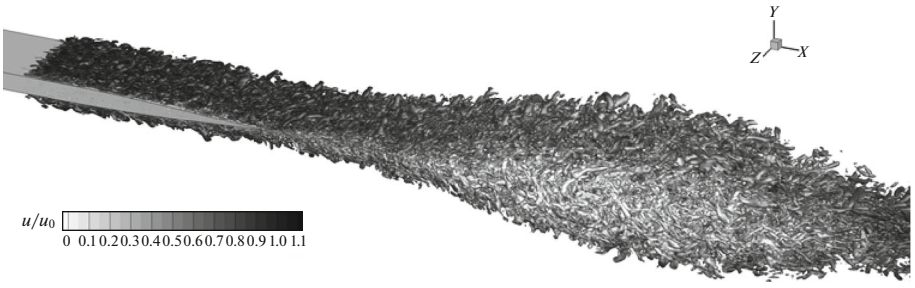

Fig. 15. Isosurface of Q-criterion colored by streamwise velocity.

flat plate boundary layer. The grid refinement results in a considerable drop of the level of subgrid viscosity, in the corresponding reduction of the size of the resolved turbulent structures, and in the growth of the extent of the inertial range of the turbulence spectrum.

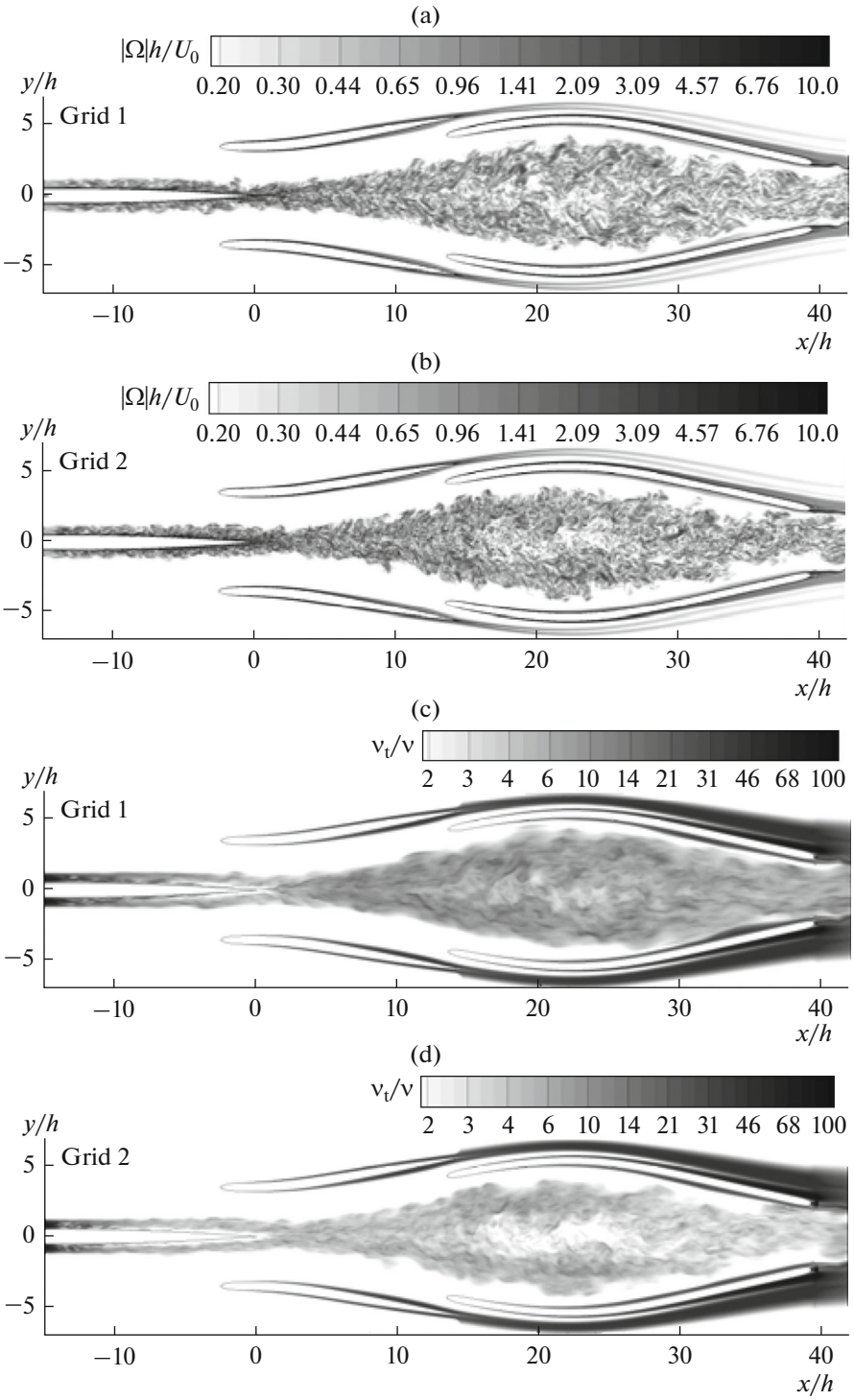

Fig. 16. Instantaneous fields of vorticity magnitude and subgrid viscosity from solution of Problem 2 on baseline (Grid 1) and refined (Grid 2) grids.

At the same time, the mean flow velocity and the statistical turbulent characteristics in the wake computed on the both, baseline and refined, grids (Grid 1 and Grid 2) are virtually identical (Figs. 18, 19), which supports high accuracy of the prediction of all these quantities.

Analysis of these results and, particularly, of the field of the mean streamwise velocity component shown in Fig. 18 suggests that at the considered geometric parameters of the Problem 2, the off-body

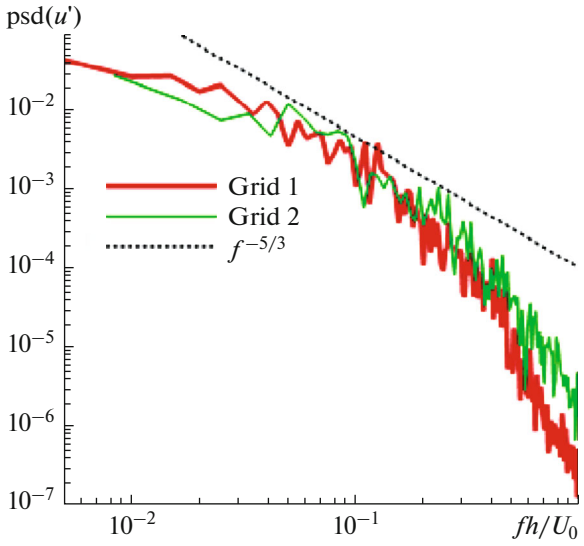

Fig. 17. Effect of grid-refinement on the turbulence spectrum in section $x/h = 15$.

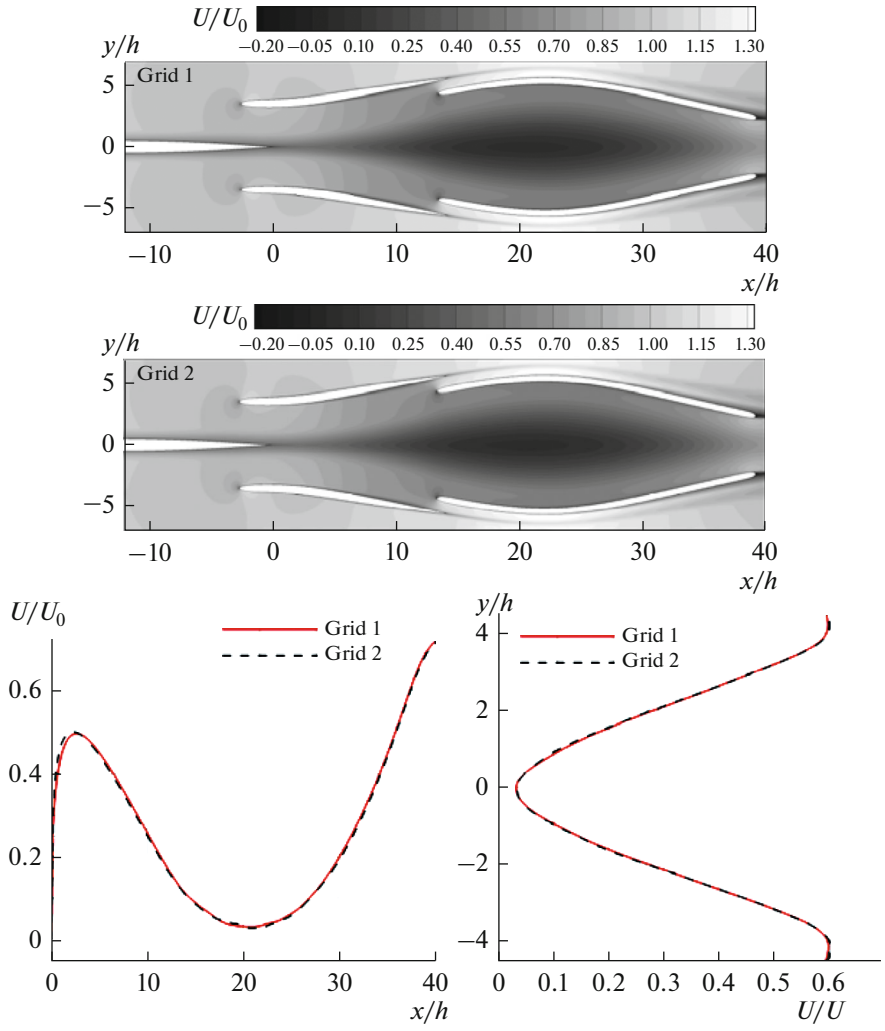

Fig. 18. Effect of grid refinement on the mean streamwise velocity field (upper frames), on its distribution along the wake symmetry plane ($y = 0$), and profile in section $x/h = 20$ (lower frames).

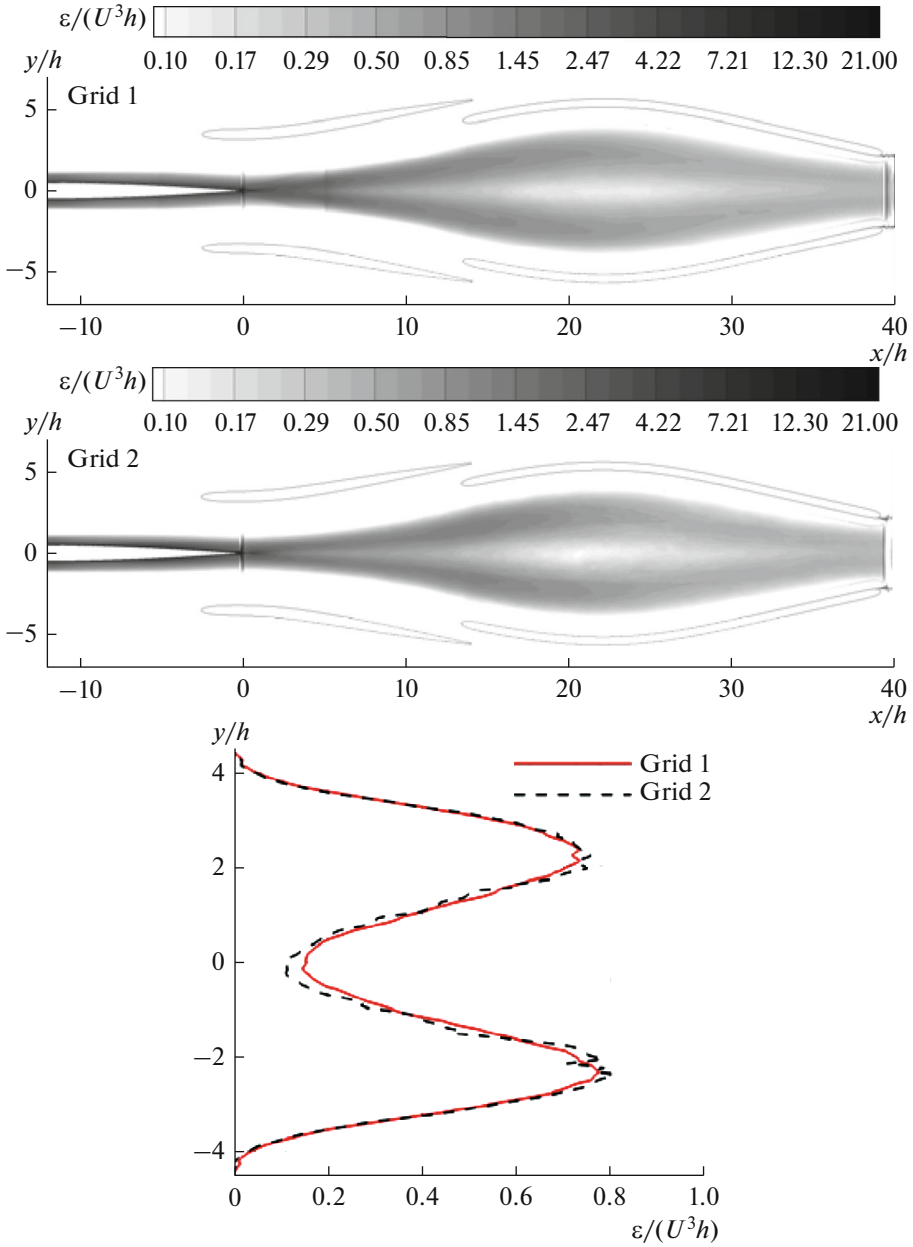

Fig. 19. Effect of grid-refinement on the field of rate of viscous dissipation of kinetic energy (upper frames) and on its profile in section $x/h = 20$ (lower frame).

recirculation zone is not formed. However, with reducing the distance between leading edges of upstream liner-foil pare and symmetry plane from 7 cm down to 5 cm (this possibility is provided by the experimental rig [7]), the APG increases and such zone shows up, independently on the Reynolds number value (Fig. 20). Considering that RANS-based prediction of the wakes in this situation is the most challenging, results of the simulation of this configuration substantially widen the validation basis for RANS models.

CONCLUSIONS

The paper presents results of numerical investigations of two turbulent wakes of the flat plate subjected to adverse pressure gradient at high (10^6–10^7) values of the Reynolds number. The study is conducted in the framework of the German–Russian project "Wake Flows in Adverse Pressure Gradient". In the first

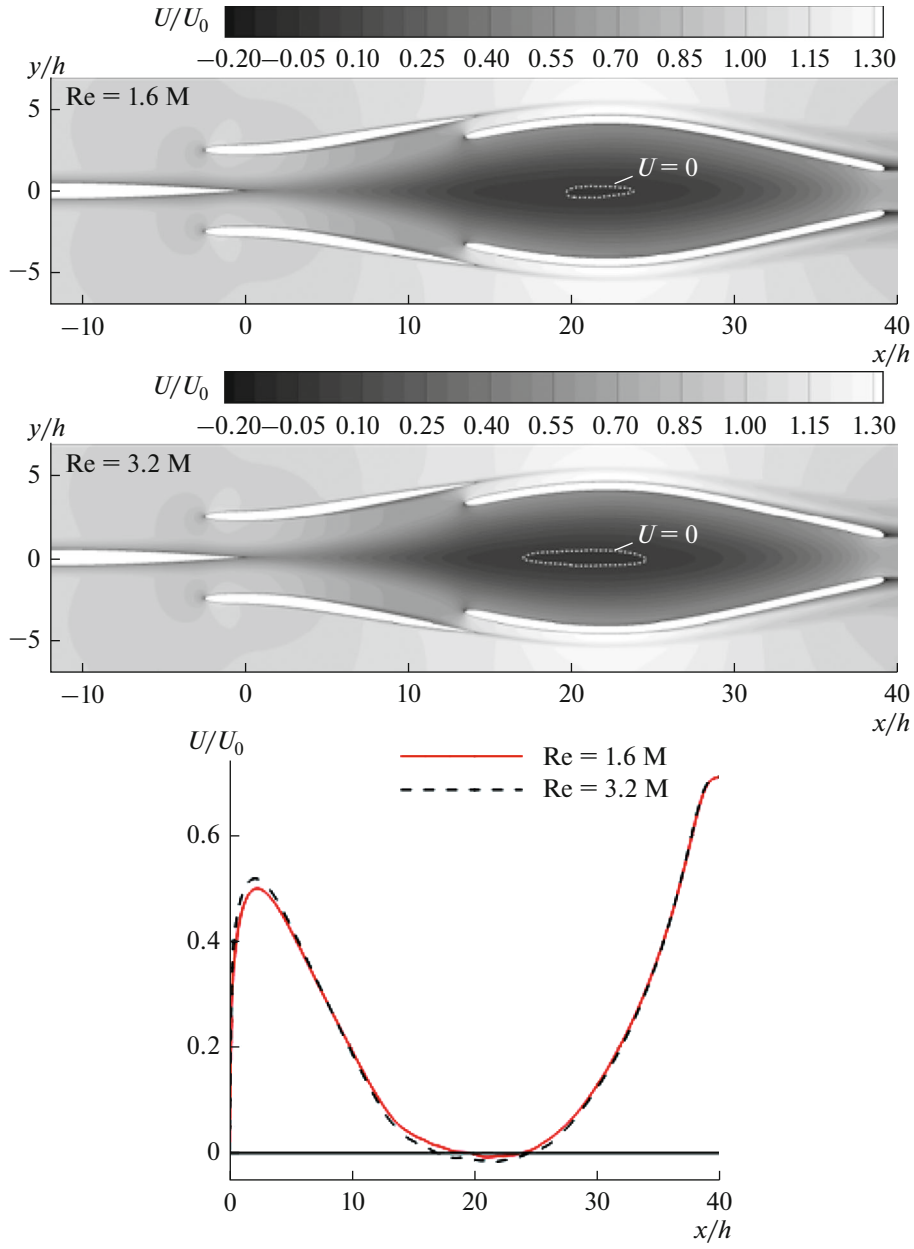

Fig. 20. Field of mean streamwise velocity and its distribution along the wake symmetry plane ($y = 0$) at reduced distance between the leading edges of upstream pair of liner foils and symmetry plane equal to 5 cm at Re = 1.6 and 3.2 million.

wake configuration, the pressure gradient is created by a plane diffusor located downstream of the plate, while in the second one, it is generated by a specially designed system of two pairs of thin liner foils.

The simulations are performed with the use of the zonal RANS-IDDES model. The RANS modeling is applied for the computation of the boundary layer on the upstream part of the plate, and the IDDES approach is used for computing the remaining (downstream) part of this boundary layer (in this area the IDDES functions as LES with wall modeling) and the wake where the IDDES performs in a pure LES mode. For creating turbulent content at the inlet of the IDDES subdomain, the Volume Synthetic Turbulence Generator is used. The high accuracy of the simulations is supported by a weak sensitivity of their results to grid refinement.

It is shown that in the both considered configurations, adverse pressure gradient leads to a significant stagnation of the wake (the velocity in its symmetry plane drops to zero or even becomes negative), which

is typical of the wakes of the elements of the high-lift wings at take-off and landing regimes. Detailed data are obtained on mean parameters and statistical turbulence characteristics of the considered wakes, including the rate of viscous dissipation of the turbulent kinetic energy and the components of the Reynolds stresses. Together with results of experiments which are currently performed within the project, these data constitute a comprehensive database for improvement and validation of RANS turbulence models for calculating the class of flows in question.

ACKNOWLEDGMENTS

The study was carried out in the framework of a joint German–Russian project and was funded by RBRF (Grant no. 17-58-12002). Computations were performed with the use of resources of the Supercomputer Center "Polytechnichesky".

REFERENCES

1. C. L. Rumsey, J. P. Slotnick, and A. J. Sclafani, "Overview and summary of the Third AIAA High Lift Prediction Workshop," AIAA Paper, AIAA-2018-1258 (2018); J. Aircr. **56** (2), 621–644 (2019).
2. D. M. Driver and G. G. Mateer, "Wake flow in adverse pressure gradient," Int. J. Heat Fluid Flow **23** (5), 564–571 (2002).
3. M. J. Tummers, K. Hanjalić, D. M. Passchier, and R. A. W. M. Henkes, "Computations of a turbulent wake in a strong adverse pressure gradient," Int. J. Heat Fluid Flow **28** (3), 418–428 (2007).
4. M. L. Shur, P. R. Spalart, M. Kh. Strelets, and A. K. Travin, "A hybrid RANS-LES approach with delayed-DES and wall-modelled LES capabilities," Int. J. Heat Fluid Flow **29** (6), 1638–1649 (2008).
5. M. Shur, M. Strelets, A. Travin, et al., "Improved embedded approaches," in *Go4Hybrid*: *Grey Area Mitigation for Hybrid RANS-LES Methods*, Ed. by C. Mockett, W. Haase, and D. Schwamborn, Notes on Numerical Fluid Mechanics and Multidisciplinary Design, (Springer, Cham, 2017), Vol. 134, pp. 51–87.
6. F. R. Menter, "Two-equation eddy-viscosity turbulence models for engineering applications," AIAA J. **32** (8), 1598–1605 (1994).
7. W. Breitenstein, P. Scholz, R. Radespiel, et al, "A wind tunnel experiment for symmetric wakes in adverse pressure gradients," AIAA Paper, AIAA-2019-1875 (2019).
8. M. Shur, M. Strelets, and A. Travin. "High-order implicit multi-block Navier-Stokes code: Ten-years experience of application to RANS/DES/LES/DNS of turbulent flows," Invited Lecture, in *7th Symposium on Overset Composite Grids and Solution Technology, Huntington Beach, CA, USA, October 5–7, 2004*. http://cfd.spbstu.ru/agarbaruk/c/document_library/DLFE-42505.pdf.
9. S. E. Rogers and D. Kwak, "An upwind differencing scheme for the time accurate incompressible Navier-Stokes equations," AIAA J. **28** (2), 253–262 (1990).
10. A. Dejoan and M. A. Leschziner, "Large eddy simulation of a plane turbulent wall jet," Phys. Fluids **17** (2), 025102 (2005).
https://doi.org/10.1063/1.1833413